

Radiative Transfer in Accretion Disk Winds

Jun FUKUE

Astronomical Institute, Osaka Kyoiku University, Asahigaoka, Kashiwara, Osaka 582-8582
fukue@cc.osaka-kyoiku.ac.jp

(Received 0 0; accepted 0 0)

Abstract

Radiative transfer equation in an accretion disk wind is examined analytically and numerically under the plane-parallel approximation in the subrelativistic regime of $(v/c)^1$, where v is the wind vertical velocity. Emergent intensity is analytically obtained for the case of a large optical depth, where the flow speed and the source function are almost constant. The usual limb-darkening effect, which depends on the direction cosine at the zero-optical depth surface, does not appear, since the source function is constant. Because of the vertical motion of winds, however, the emergent intensity exhibits the *velocity-dependent* limb-darkening effect, which comes from the Doppler and aberration effects. Radiative moments and emergent intensity are also numerically obtained. When the flow speed is small ($v \leq 0.1c$), the radiative structure resembles to that of the static atmosphere, where the source function is proportional to the optical depth, and the usual limb-darkening effect exists. When the flow speed becomes large, on the other hand, the flow speed attains the constant terminal one, and the velocity-dependent limb-darkening effect appears. We thus carefully treat and estimate the wind luminosity and limb-darkening effect, when we observe an accretion disk wind.

Key words: accretion, accretion disks — galaxies: active — radiative transfer — relativity — X-rays: stars

1. Introduction

Accretion disks are now widely believed to be energy sources in various active phenomena in the universe: in protoplanetary nebulae around young stellar objects (YSOs), in cataclysmic variables (CVs) and supersoft X-ray sources (SSXSs), in galactic X-ray binaries and microquasars (μ QSOs), and in active galaxies (ANGs) and quasars (QSOs). Accretion-disk models have been extensively studied during these three decades (see Kato et al. 1998 for a review). Besides the traditional standard disk by Shakura and Sunayev (1973), new type disks, such as advection-dominated accretion flows (ADAF) or radiatively-inefficient accretion flows (RIAF) for the very small mass-accretion rate (e.g., Narayan, Yi 1994), and supercritical accretion disks or so-called slim disks for the very large mass-accretion rate (e.g., Abramowicz et al. 1988).

Accretion disk winds have been also extensively examined in relation to astrophysical jets and outflows: in bipolar outflows from YSOs, in mass outflows from CVs and SSXSs, in relativistic jets from μ QSOs, AGNs, QSOs, and in gamma-ray bursts (GRBs). In particular, intense radiation fields of luminous supercritical accretion disks may be responsible for relativistic jets from super-Eddington sources, such as luminous μ QSOs, GRS 1915+105 and SS 433, luminous QSOs, 3C 273, and energetic GRBs (see, e.g., Fukue 2004 for references).

In such circumstances, radiative transfer in accretion disk winds as well as accretion disks becomes more and more important.

Radiative transfer in the standard disk has been investigated in relation to the structure of a static disk atmosphere and the spectral energy distribution from the disk surface (e.g., Meyer, Meyer-Hofmeister 1982; Cannizzo, Wheeler 1984). Furthermore, gray and non-gray models of accretion disks were constructed under numerical treatments (Křiž and Hubeny 1986; Shaviv and Wehrse 1986; Adam et al. 1988; Mineshige, Wood 1990; Ross et al. 1992; Shimura and Takahara 1993; Hubeny, Hubeny 1997, 1998; Hubeny et al. 2000, 2001; Davis et al. 2005; Hui et al. 2005) and under analytical ones (Hubeny 1990; Artemova et al. 1996; Fukue, Akizuki 2006a).

Radiative transfer in the accretion disk wind, on the other hand, has not been well considered both in the non-relativistic and relativistic regimes. Recently, radiative transfer in a moving disk atmosphere was firstly investigated in the subrelativistic regime (Fukue 2005a, 2006a), and in the relativistic regime (Fukue 2005b, 2006b; Fukue, Akizuki 2006b). In contrast to the static atmosphere, in the moving atmosphere the boundary condition at the surface of zero optical depth should be modified (Fukue 2005a, b). Moreover, the usual Eddington approximation violates in the highly relativistic flow (Fukue 2005b; see also Turolla, Nobili 1988; Nobili et al. 1991; Turolla et al. 1995; Dullemond 1999), and the velocity-dependent variable Eddington factor was proposed (Fukue 2006b for a plane-parallel case; Akizuki, Fukue 2007 for a spherical case).

Radiation hydrodynamical (RHD) simulations were also performed for radiation-dominated supercritical disks with winds by several researchers (Eggum et al. 1985,

1988; Okuda et al. 1997, 2005; Okuda, Fujita 2000; Okuda 2002; Ohsuga et al. 2005; Ohsuga 2006). In these current studies of RHD simulations for disks and winds, they were done in the subrelativistic regime up to the order of $(v/c)^1$, using the moment formalism and the flux-limited diffusion (FLD) approximation (Levermore, Pomraning 1981). The flux-limited diffusion method provides good approximations to the exact solutions but only if they are derived from transfer equations in which terms of the order of $(v/c)^2$ or higher have been retained (Yin, Miller 1995).

Radiative transfer problems on accretion disks and winds are not well understood yet, in particular for the relativistic cases. Hence, in order to clarify the physics, in addition to RHD simulations, we must treat the simplified problem in the analytical way.

In this paper, we thus examine radiative transfer in the accretion disk wind, which is assumed to blow off from the luminous disk in the vertical direction (plane-parallel approximation), and analytically and numerically obtain the flow solutions for the case without internal heating. In the previous studies, radiative flows in the vertically moving atmosphere were solved in the subrelativistic regime (Fukue 2005a, 2006a), and in the relativistic regime (Fukue 2005b, 2006b; Fukue, Akizuki 2006b), where only radiative moments were obtained. In the present paper, we further obtain the radiation intensity as well as radiative moments.

In the next section we describe the basic equations. In section 3, we show analytical solutions, while we present numerical solutions in section 4. The final section is devoted to concluding remarks.

2. Basic Equations

Let us suppose a luminous flat disk, deep inside which gravitational or nuclear energy is released via viscous heating or other processes. The radiation energy is transported in the vertical direction, and the disk gas, itself, also moves in the vertical direction as a *disk wind* due to the action of radiation pressure (i.e., plane-parallel approximation). For simplicity, in the present paper, the radiation field is considered to be sufficiently intense that both the gravitational field of, e.g., the central object and the gas pressure can be ignored. We also assume the gray approximation, where the opacities do not depend on the frequency. As for the order of the flow velocity v , we consider the subrelativistic regime, where the terms of the first order of (v/c) are retained, in order to take account of radiation drag.

The radiative transfer equations are given in several literatures (Chandrasekhar 1960; Mihalas 1970; Rybicki, Lightman 1979; Mihalas, Mihalas 1984; Shu 1991; Kato et al. 1998). For the plane-parallel geometry in the vertical direction (z), the radiation hydrodynamic equations are described as follows (Kato et al. 1998). It should be noted that the basic equations below are the same as those given in Fukue (2005a), except for the transfer equation for the radiation intensity.

For matter, the continuity equation is

$$\rho v = J \quad (= \text{const.}), \quad (1)$$

where ρ is the gas density, v the vertical velocity, and J the mass-loss rate per unit area. The equation of motion is

$$v \frac{dv}{dz} = \frac{\kappa_{\text{abs}} + \kappa_{\text{sca}}}{c} [F - (E + P)v], \quad (2)$$

where κ_{abs} and κ_{sca} are the absorption and scattering opacities (gray), which are defined in the comoving (fluid) frame, E the radiation energy density, F the radiative flux, and P the radiation pressure in the vertical direction, which are measured in the fixed (laboratory) frame. In a gas-pressureless approximation, the energy equation is reduced to

$$0 = q^+ - \rho \left(j - c\kappa_{\text{abs}}E + \kappa_{\text{abs}} \frac{2Fv}{c} \right), \quad (3)$$

where q^+ is the heating and j is the emissivity, which is measured in the comoving frame.

For radiation fields, the frequency-integrated transfer equation, the zeroth moment equation, and the first moment equation become, respectively,

$$\mu \frac{dI}{dz} = \rho \left[(1 + 3\beta\mu) \frac{j}{4\pi} - (\kappa_{\text{abs}} + \kappa_{\text{sca}})(1 - \beta\mu)I + \frac{\kappa_{\text{sca}}}{4\pi} \{ (1 + 3\beta\mu)cE - 2F\beta \} \right], \quad (4)$$

$$\frac{dF}{dz} = \rho (j - c\kappa_{\text{abs}}E + \kappa_{\text{abs}}F\beta - \kappa_{\text{sca}}F\beta), \quad (5)$$

$$\frac{dP}{dz} = \frac{\rho}{c} [j\beta - (\kappa_{\text{abs}} + \kappa_{\text{sca}})F + \kappa_{\text{abs}}cP\beta + \kappa_{\text{sca}}(cE + cP)\beta], \quad (6)$$

where μ is $\cos\theta$, θ being the polar angle, and $\beta = v/c$. We further adopt the Eddington approximation in the comoving frame, which is transformed into

$$P = \frac{1}{3}E + \frac{4}{3}\frac{F}{c}\beta \quad (7)$$

in the fixed frame (Kato et al. 1998). Here, the transfer equation (4) is corrected to the order of $(v/c)^1$ (Kato et al. 1998).

Eliminating j with the help of equation (3), and introducing the optical depth by

$$d\tau = -(\kappa_{\text{abs}} + \kappa_{\text{sca}})\rho dz, \quad (8)$$

we can rearrange the basic equations up to the order of $(v/c)^1$ as

$$c^2 J \frac{d\beta}{d\tau} = -(F - 4cP\beta), \quad (9)$$

$$\mu \frac{dI}{d\tau} = -\frac{1}{4\pi} \frac{q^+}{(\kappa_{\text{abs}} + \kappa_{\text{sca}})\rho} (1 + 3\beta\mu) + (1 - \beta\mu)I - (1 + 3\beta\mu) \frac{1}{4\pi} (cE - 2F\beta), \quad (10)$$

$$\frac{dF}{d\tau} = -\frac{q^+}{(\kappa_{\text{abs}} + \kappa_{\text{sca}})\rho} + F\beta, \quad (11)$$

$$c \frac{dP}{d\tau} = -\frac{q^+}{(\kappa_{\text{abs}} + \kappa_{\text{sca}})\rho} \beta + F - 4cP\beta, \quad (12)$$

$$J \frac{dz}{d\tau} = - \frac{1}{(\kappa_{\text{abs}} + \kappa_{\text{sca}})} c\beta. \quad (13)$$

Finally, integrating the sum of equations (9) and (12) gives the momentum flux conservation in the present approximation,

$$c^2 J\beta + cP = cP_0 - \int \frac{q^+}{(\kappa_{\text{abs}} + \kappa_{\text{sca}})\rho} \beta d\tau = cP_0, \quad (14)$$

when there is no heating ($q^+ = 0$). In addition, the subscript 0 means the value at some reference position (i.e., the wind base). Similarly from equations (9) and (11) we have the energy flux conservation,

$$\frac{1}{2} Jv^2 + F = F_0 - \int \frac{q^+}{(\kappa_{\text{abs}} + \kappa_{\text{sca}})\rho} d\tau = F_0, \quad (15)$$

when there is no heating ($q^+ = 0$). Here, the first term on the left-hand side is eventually dropped, although we retain it here to clarify the physical meanings.

We solve equations (9), (14), (15), and (10) for appropriate boundary conditions, and we obtain analytic solutions.

As for the boundary conditions at the wind base of $\tau = \tau_0$ and at the wind top of $\tau = 0$, we impose the following conditions.

At the wind base on the disk surface with an arbitrary optical depth τ_0 , the flow velocity β is zero, the radiative flux is F_0 (which is a measure of the strength of radiation field), and the radiation pressure is P_0 (which connects with the radiation pressure gradient), where the subscript 0 denotes the values at the wind base.

At the wind top, on the other hand, as already pointed out in Fukue (2005b), the usual boundary conditions for the static atmosphere cannot be used for the present radiative wind, which moves with velocity at the order of the speed of light. Namely, the radiation field just above the wind top changes when the gas itself does move upward, since the direction and intensity of radiation change due to relativistic aberration and Doppler effect (cf. Kato et al. 1998; Fukue 2000). If a flat infinite plane with surface intensity I_s in the comoving frame is not static, but moving upward with a speed v_s ($= c\beta_s$, and the corresponding Lorentz factor is γ_s), where the subscript s denotes the values at the surface, then, just above the surface, the radiation energy density E_s , the radiative flux F_s , and the radiation pressure P_s measured in the inertial frame become, respectively,

$$cE_s = 2\pi I_s \frac{3\gamma_s^2 + 3\gamma_s u_s + u_s^2}{3}, \quad (16)$$

$$F_s = 2\pi I_s \frac{3\gamma_s^2 + 8\gamma_s u_s + 3u_s^2}{6}, \quad (17)$$

$$cP_s = 2\pi I_s \frac{\gamma_s^2 + 3\gamma_s u_s + 3u_s^2}{3}, \quad (18)$$

where u_s ($= \gamma_s v_s / c$) is the flow four velocity at the surface (Fukue 2005b). As a result, we have the boundary condition at the wind top within the present approximation,

$$\frac{cP_s}{F_s} = \frac{2 + 6\beta_s + 6\beta_s^2}{3 + 8\beta_s + 3\beta_s^2} \sim \frac{2}{3} + \frac{2}{9}\beta_s. \quad (19)$$

This is the consistent boundary condition under the present subrelativistic regime up to the order of $(v/c)^1$, although Fukue (2005a) have approximately used the boundary condition, $cP_s/F_s = 2/3$, for a static atmosphere. In general, at the wind top of $\tau = 0$, the boundary condition (19) is not satisfied. Hence, for given parameters, we adjust and obtain the mass-loss rate J as an eigen value, so as to satisfy the boundary condition (19).

As already stated, for the internal heating in the wind, we assume that there is no heating source ($q^+ = 0$), although it is straightforward to extend the model to the case with heating. On the other hand, at the wind base on the luminous disk, there is assumed to be a uniform source of I_0 .

3. Analytical Solutions

In Fukue (2005a), analytical solutions for radiative moments were already derived. For the completeness, in this section, we first recalculate them under the consistent boundary condition. Using the analytical expressions for moments, we then calculate the radiative intensity, which we wish to know in the present paper.

3.1. Flow Velocity and Radiative Moments

Under the present subrelativistic regime, equation (15) means that the radiative flux F is conserved:

$$F = F_0 = F_s. \quad (20)$$

Using the boundary conditions at the wind base ($v = 0$), equation (14) is expressed as

$$Jv + P = P_0. \quad (21)$$

Hence, equation (9) becomes

$$cJ \frac{dv}{d\tau} = -(F_s - 4P_0v), \quad (22)$$

that can be analytically solved to yield

$$v = \frac{F_s}{4P_0} \left[1 - e^{-\frac{4P_0}{cJ}(\tau - \tau_0)} \right]. \quad (23)$$

Thus, the radiative flow from the luminous disk without heating is expressed in terms of the boundary values and the mass-loss rate. In addition, the flow velocity v_s at the wind top ($\tau = 0$) is

$$v_s = \frac{F_s}{4P_0} \left(1 - e^{-\frac{4P_0}{cJ}\tau_0} \right). \quad (24)$$

Using the boundary condition at the wind top, we further impose a condition on the values at boundaries. Inserting boundary values (19) into momentum equation (21), using equation (23), we have the following relation:

$$\frac{cP_0}{F_s} = \frac{2}{3} + \left(\frac{cJ}{4P_0} + \frac{F_s}{18cP_0} \right) \left(1 - e^{-\frac{4P_0}{cJ}\tau_0} \right). \quad (25)$$

That is, for given τ_0 and P_0 at the wind base, the mass-loss rate J is determined in units of F_s/c^2 , as an eigen

value. Compared with Fukue (2005a), the second term in the first parentheses on the right-hand side is an additional one, which appears due to the present corrected boundary condition (19).

As already stated in Fukue (2005a), the mass-loss rate increases as the initial radiation pressure increases, while the flow terminal speed increases as the initial radiation pressure and the loaded mass decrease.

Moreover, as easily shown from equation (25), in order for the flow to exist, the radiation pressure P_0 at the flow base is restricted in some range,

$$\frac{2 + \sqrt{6}}{6} < \frac{cP_0}{F_s} < \frac{2}{3} + \tau_0, \quad (26)$$

which is slightly modified from that given in Fukue (2005a), due to the corrected boundary condition. At the upper limit of $cP_0/F_s = 2/3 + \tau_0$, the loaded mass diverges and the flow terminal speed becomes zero. On the other hand, at the lower limit of $cP_0/F_s = (2 + \sqrt{6})/6$, the pressure gradient vanishes, the loaded mass becomes zero and the terminal speed approaches the saturation speed of

$$\beta_\infty = \frac{-6 + 3\sqrt{6}}{4} \sim 0.337, \quad (27)$$

where the radiative flux F is balanced by the radiation drag $4P_0v$ with the boundary condition (19).

In figure 1 we show analytical solutions, the flow velocity v (solid curves) in units of c , the radiation pressure P (dashed ones) in units of F_s/c , and the source function S (chain-dotted ones) in units of F_s as a function of the optical depth τ for several values of P_0 at the wind base in a few cases of τ_0 .

When the initial radiation pressure P_0 at the wind base is large, the pressure gradient between the wind base and the wind top is also large. As a result, the loaded mass J also becomes large, but the flow final speed v_s is small due to momentum conservation (14). When the initial radiation pressure P_0 is small, on the other hand, the pressure gradient becomes small, and the loaded mass is also small, but the flow final speed becomes large. In the latter case, the source function S becomes almost constant.

Within the present approximation of $(v/c)^1$ with the boundary condition (19), the flow final speed saturates at $0.337 c$.

3.2. Emergent Intensity

Now, we turn to the transfer equation (10), or

$$\mu \frac{dI}{d\tau} = (1 - \beta\mu)I - (1 + 3\beta\mu) \frac{1}{4\pi} (cE - 2F\beta), \quad (28)$$

when there is no heating.

Under the present approximation up to the order of $(v/c)^1$, F is constant, but E (P) and β are generally functions of τ . If, however, the radiation field is sufficiently intense, the wind flow quickly saturates; the radiative flux, F , is balanced by the radiation drag force, $(E + P)v$, and the wind speed reaches the saturation terminal one, $F/(E + P)$. In such a case, the wind speed and the radiation quantities are almost constant. In other words, the

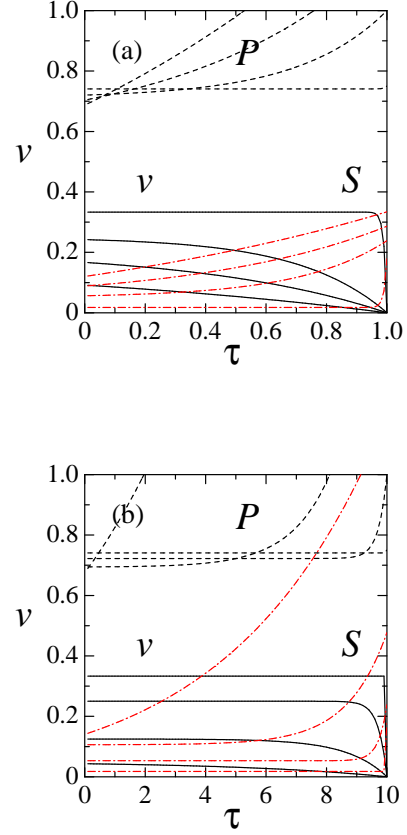


Fig. 1. Flow velocity v (solid curves) in units of c , radiation pressure P (dashed ones) in units of F_s/c , and source function S in units of F_s (chain-dotted ones) as a function of the optical depth τ for several values of P_0 at the wind base in a few cases of τ_0 : (a) $\tau_0 = 1$ and (b) $\tau_0 = 10$. From top to bottom of v and from bottom to top of P and S , the values of P_0 are 0.75, 1, 1.2, 1.4 in (a), and 0.75, 1, 2, 5 in (b).

source function, the second term on the right-hand side of equation (28), is almost constant (see figure 1), since in the present case the source function S is expressed as

$$S = \frac{cE - 2F\beta}{4\pi} = \frac{3cP - 6F\beta}{4\pi}. \quad (29)$$

Here, we thus assume that the wind velocity is constant, and analytically integrate the transfer equation (28).

When the wind velocity becomes a constant terminal one, using equations (23), (21), and (7), we have

$$\beta = \beta_s = \frac{F_s}{4cP_0}, \quad (30)$$

$$cP = cP_0 - c^2J\beta = \frac{2}{3}F_s + \frac{1}{18} \frac{F_s^2}{cP_0}, \quad (31)$$

$$cE = 3cP - 4F\beta = 2F_s - \frac{5}{6} \frac{F_s^2}{cP_0}. \quad (32)$$

Hence,

$$cE - 2F\beta = 2F_s - \frac{4}{3} \frac{F_s^2}{cP_0} = 2F_s - \frac{16}{3} F_s\beta. \quad (33)$$

That is, the source function measured in the fixed frame slightly decreases due to the effect of the relativistic motion.

Under the above situations, we can now integrate the radiative transfer equation (28), similar to Fukue and Akizuki (2006). After several partial integrations, we obtain both an outward intensity $I(\tau, \mu)$ ($\mu > 0$) and an inward intensity $I(\tau, -\mu)$ as

$$I(\tau, \mu) = \frac{cE - 2F\beta}{4\pi} \frac{1 + 3\beta\mu}{1 - \beta\mu} \left[1 - e^{-\frac{1-\beta\mu}{\mu}(\tau-\tau_0)} \right] + I(\tau_0, \mu) e^{-\frac{1-\beta\mu}{\mu}(\tau-\tau_0)}, \quad (34)$$

$$I(\tau, -\mu) = \frac{cE - 2F\beta}{4\pi} \frac{1 + 3\beta\mu}{1 - \beta\mu} \left[1 - e^{-\frac{1-\beta\mu}{\mu}\tau} \right], \quad (35)$$

where $I(\tau_0, \mu)$ is the boundary value at the wind base on the luminous disk.

In general case with finite optical depth τ_0 and uniform incident intensity I_0 from the disk, the boundary value $I(\tau_0, \mu)$ of the outward intensity I consists of two parts:

$$I(\tau_0, \mu) = I_0 + I(\tau_0, -\mu), \quad (36)$$

where I_0 ($= F_s/\pi$) is the uniform incident intensity and $I(\tau_0, -\mu)$ is the *inward* intensity from the backside of the disk beyond the midplane. Determining $I(\tau_0, -\mu)$ from equation (35), we finally obtain the outward intensity as

$$I(\tau, \mu) = \frac{cE - 2F\beta}{4\pi} \frac{1 + 3\beta\mu}{1 - \beta\mu} \left[1 - e^{-\frac{1-\beta\mu}{\mu}(\tau-2\tau_0)} \right] + I_0 e^{-\frac{1-\beta\mu}{\mu}(\tau-\tau_0)}, \\ \sim \frac{3F_s}{4\pi} \left\{ \left(\frac{2}{3} - \frac{16}{9}\beta + \frac{8}{3}\beta\mu \right) \left[1 - e^{-\frac{1-\beta\mu}{\mu}(\tau-2\tau_0)} \right] + \frac{4}{3} e^{-\frac{1-\beta\mu}{\mu}(\tau-\tau_0)} \right\}, \quad (37)$$

where we have used $F_s = \pi I_0$.

Finally, the emergent intensity $I(0, \mu)$ emitted from the wind top becomes

$$I(0, \mu) = \frac{3F_s}{4\pi} \left[\left(\frac{2}{3} - \frac{16}{9}\beta + \frac{8}{3}\beta\mu \right) \left(1 - e^{-\frac{1-\beta\mu}{\mu}2\tau_0} \right) + \frac{4}{3} e^{-\frac{1-\beta\mu}{\mu}\tau_0} \right], \\ \sim \frac{3F_s}{4\pi} \left(\frac{2}{3} - \frac{16}{9}\beta + \frac{8}{3}\beta\mu \right) \quad \text{for large } \tau_0. \quad (38)$$

Under the present approximation, where the source function is constant, the usual limb darkening does not appear: e.g., $(3F_s/4\pi)(2/3 + \tau)$ for the Milne-Eddington solution. Due to the Doppler and aberration effects originating from the vertical motion of winds, however, the emergent intensity (38) depends on the wind velocity as well as the direction cosine. This is the *velocity-dependent* limb-darkening effect.

In figure 2, the emergent intensity $I(0, \mu)$ normalized by the isotropic value \bar{I} ($= F_s/\pi$) is shown for several values of β as a function of μ . Although the present approximation may be valid for $\beta \leq 0.1$, we show the cases for $\beta \leq 0.3$ in order to stress the velocity-dependency.

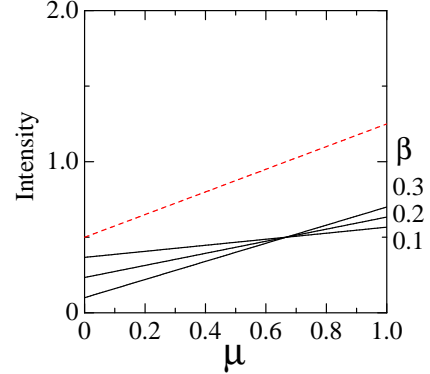


Fig. 2. Normalized emergent intensity as a function of μ for the case without heating. The numbers attached on each curve are values of β of wind velocity. The dashed straight line is for the usual Milne-Eddington solution for the plane-parallel case.

As is easily seen in figure 2, as the velocity becomes large, the limb-darkening effect becomes prominent. That is, the emergent intensity increases in the poleward direction, while it decreases in the edgeward direction. As a result, a wind luminosity would be overestimated by a pole-on observer and underestimated by an edge-on observer, when we observe an optically-thick accretion disk wind.

It is interesting that the intensity does not change in the direction of $\mu = 2/3$.

4. Numerical Solutions

In this section, we numerically solve equations (9) and (12) [or (14)] with constant F , and further solve equation (10) [or (28)] for several cases, and compare the results with that of analytical solutions to check the accuracy and limitations of analytical solutions.

4.1. Flow Velocity and Radiative Moments

In figure 3 we show several numerical solutions, the flow velocity v (thick solid curves) in units of c and the radiation pressure P (thick dashed curves) in units of F_s/c as a function of the optical depth τ for several values of P_0 at the wind base in a few cases of τ_0 . Corresponding analytical solutions are shown by thin curves, although the mass-loss rates are slightly different so as to satisfy the upper boundary condition (19).

As is seen in figure 3, in both analytical and numerical cases, when the initial pressure P_0 and the loaded mass are large, the flow speed is small ($v \leq 0.1c$). In such a case, the radiative structure resembles to that of the static atmosphere, where the source function is proportional to the optical depth. When the initial pressure and the loaded mass decrease, on the other hand, the flow speed becomes large to attain the saturation one. In such a case, the source function is almost constant.

In addition, for the same parameters the analytical

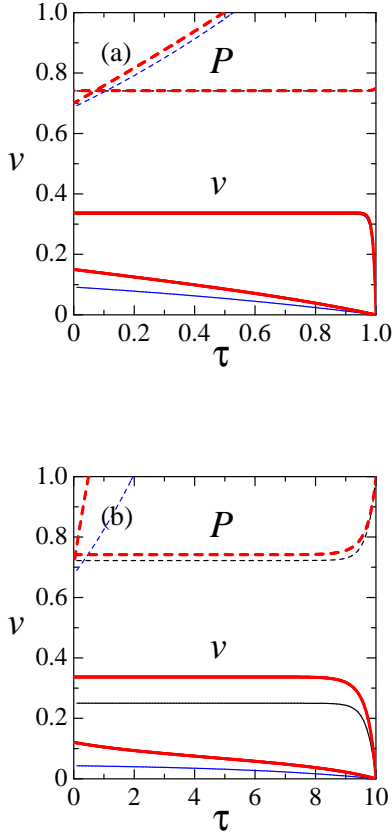


Fig. 3. Flow velocity v (thick solid curves) in units of c and radiation pressure P (thick dashed curves) in units of F_s/c as a function of the optical depth τ for several values of P_0 at the wind base in a few cases of τ_0 : (a) $\tau_0 = 1$ and (b) $\tau_0 = 10$. From top to bottom of v and from bottom to top of P , the values of P_0 are 0.75 and 1.4 in (a), and 1 and 5 in (b). Corresponding analytical solutions are shown by thin curves.

and numerical solutions are slightly different, although we have solved the same basic equations. This is understood as follows. Our basic equations are up to the order of $(v/c)^1$, and therefore have the accuracy of the same order. In deriving the analytical solutions, we have dropped the terms of order of $(v/c)^2$, while we have retained those terms in solving the numerical solutions. Hence, the analytical and numerical solutions should be same within the accuracy of $(v/c)^1$.

4.2. Emergent Intensity

After obtaining the numerical solutions for v and P (i.e., E), we can further numerically integrate the transfer equation (28) for many angles μ as a function of τ under appropriate boundary conditions and given initial conditions of τ_0 and P_0 . As boundary conditions, we set a uniform source of I_0 at the wind base, while there is no incident intensity at the wind top: $I^+(\tau_0, \mu) = I_0 + I^-(\tau_0, -\mu)$ and $I^-(\tau_0, -\mu) = 0$. We use meshes of 100 for μ and 500 for τ . Finally, the emergent intensity $I(0, \mu)$ emitted from the wind top is numerically obtained as a function of angle

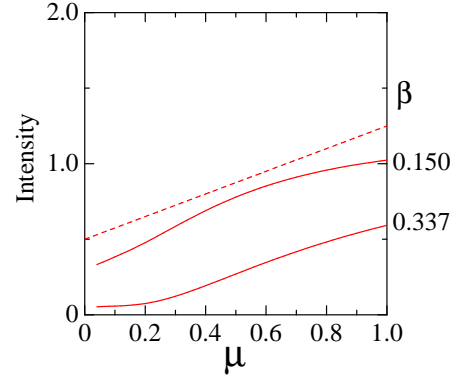


Fig. 4. Normalized emergent intensity as a function of μ for the case without heating. The numbers attached on each curve are values of β_s of wind terminal velocity. The initial optical depth τ_0 is 1 and the initial pressure P_0 is 1.4 ($\beta_s = 0.150$) and 0.75 ($\beta_s = 0.337$).

for given τ_0 and P_0 . Examples of the results are shown in figure 4.

In figure 4, the emergent intensity obtained numerically is shown for the initial optical depth of $\tau_0 = 1$, and for several values of β_s , that is attached on each curve. When the terminal speed is small, as already stated, the wind structure resembles to that of the static atmosphere. In the present case, however, the optical depth of wind is finite. As a result, at around $\mu \sim 1$ the emergent intensity is almost constant with the values of I_0 (i.e., the peaking effect diminishes), while the usual limb-darkening effect recovers for small μ , where the line-of-sight length is long.

When the terminal speed is large, on the other hand, the velocity-dependent limb-darkening effect appears again for the numerical solutions. That is to say, as stated in figure 2, due to the Doppler and aberration effects originating from the vertical motion of winds, the emergent intensity depends on the wind velocity as well as the direction cosine. In particular, the emergent intensity is enhanced and increases as μ increases.

By the way, in figure 4 the emergent intensity entirely decreases for all μ as the velocity increases. Apparently, this seems to be curious, because the relativistic boosts work in the regime with large velocity. The reason is also the relativistic effect. The present subrelativistic flow up to the order of $(v/c)^1$, the momentum and energy of radiation fields accelerate the flow. Although the flux F is conserved within the present order of $(v/c)^1$, the radiation intensity diminishes due to the interaction between the field and the flow [the $2F\beta$ term in the second term on the right-hand side of equation (28)]. In other words, the source term effectively decreases. As a result, the emergent intensity entirely decreases, compared with the non-relativistic case.

We here briefly check the consistency of the numerical results. In order to obtain the radiation intensity I from equation (28), we use the radiation energy density E_{mom} and the radiative flux $F_{\text{mom}} (= F_s)$ obtained from the mo-

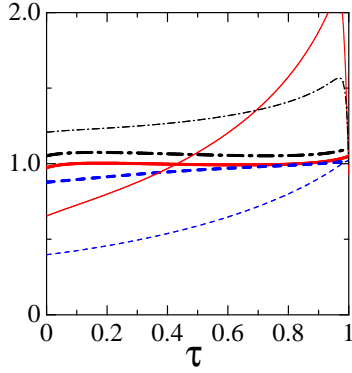


Fig. 5. Ratios between the quantities obtained from the moment equations and those obtained from the intensity. Solid curves and dashed ones denote the energy density and the flux, respectively. In the small velocity case of $\beta_s = 0.150$ (thick curves), both quantities are almost consistent. In the large velocity case of $\beta_s = 0.337$ (thin curves), on the other hand, the consistency becomes worse. In addition, chain-dotted curves mean the three times Eddington factor for the quantities obtained from the intensity.

ment equations (14). Once the radiation intensity $I(\tau, \mu)$ is obtained, we can calculate the radiation energy density E_{sim} and the radiative flux F_{sim} by the definition. If the quantities obtained from the moment equations and those obtained from the intensity coincide each other, the solutions are consistent, and vice versa.

In figure 5 we plot the ratios $E_{\text{sim}}/E_{\text{mom}}$ (solid curves) and $F_{\text{sim}}/F_{\text{mom}}$ (dashed ones) for the small velocity case of $\beta_s = 0.150$ (thick curves) and for the large velocity case of $\beta_s = 0.337$ (thin curves). In addition, we also plot the quantities $(E_{\text{sim}} + 4F_{\text{sim}}v)/(3P_{\text{sim}})$, the three times Eddington factor, by chain-dotted curves.

As is seen from figure 5, in the case of small velocity, where the structure resembles to that of the static case, the ratios are almost unity and the solutions are consistent. In the small velocity case, furthermore, the Eddington factor is almost $1/3$. In the case of large velocity, on the other hand, the ratios differ from unity. The main reason of this discrepancy is the relativistic effect. As already stated, the radiation intensity diminishes due to the interaction between the field and the flow. As a result, the intensity $I(\tau, \mu)$ as well as the emergent intensity $I(0, \mu)$ entirely decreases. Thus, F_{sim} becomes smaller than F_{mom} . Although the reason that the energy density ratio increases is less clear, it seems to be the relativistic peaking effect (Doppler boost and relativistic aberration). Indeed, the Eddington factor in the large velocity case is somewhat larger than unity. This would be also the relativistic peaking effect. Anyway, as the velocity becomes large, the consistency becomes worse, and the present treatment under the order of $(v/c)^1$ would be invalid.

5. Concluding Remarks

In this paper we have examined the radiative transfer problem in an accretion disk wind under the plane-parallel approximation in the subrelativistic regime of $(v/c)^1$. The flow velocity, the radiation pressure distribution, and other quantities are analytically and numerically solved as a function of the optical depth for the case without heating. Furthermore, the emergent intensity from the wind top with zero optical depth is also analytically obtained under the assumption of constant flow velocity, while numerically calculated.

When the source function is constant, the usual limb-darkening effect does not appear. However, the emergent intensity exhibits the *velocity-dependent* limb-darkening effect, which originates from the Doppler and aberration effects, associating with the vertical subrelativistic motion of winds. As a result, a wind luminosity would be overestimated by a pole-on observer and underestimated by an edge-on observer, when we observe an optically thick accretion disk wind.

It should be noted that the *apparent* optical depth in the relativistically moving media. Abramowicz et al. (1991) pointed out that the optical depth in the relativistic flow decreases as $\gamma(1 - \beta\mu)\tau$ toward the downstream direction, due to the Doppler and aberration effects. Inspecting equation (28) or solution (38), we find that, in the present subrelativistic flow, the optical depth τ is apparently replaced by $(1 - \beta\mu)\tau$. This is just consistent with the results by Abramowicz et al. (1991) within the order of $(v/c)^1$.

In the present modeled plane-parallel geometry, the gas density at the wind top is finite, since the wind velocity there is finite. Rigorously speaking, this situation is inconsistent with the definition of the wind top, where the optical depth is effectively zero. In more realistic cases, the disk wind would geometrically diverge, and the density quickly drops. As a result, the surface of a moving photosphere exists, even if the wind terminal velocity is finite. The present model mimics such a realistic disk wind, where the velocity-dependent limb darkening effect would also appear. In other words, as long as the acceleration of wind takes place in a small height, and then the wind diverges, the present assumption would be valid.

The radiative transfer problem investigated in the present paper must be quite *fundamental problems* for accretion disk physics and astrophysical jet formation. In this paper, for simplicity, we only considered the subrelativistic case of $(v/c)^1$. The fully relativistic case of $(v/c)^2$ will be explored in the future.

The author would like to thank an anonymous referee for valuable comments. This work has been supported in part by a Grant-in-Aid for Scientific Research (18540240 J.F.) of the Ministry of Education, Culture, Sports, Science and Technology.

References

- Abramowicz, M. A., Czerny, B., Lasota, J. P., & Szuszkiewicz, E. 1988, *ApJ*, 332, 646
- Abramowicz, M. A., Novilcov, I. D., & Pacyński B. 1991, *ApJ*, 369, 175
- Adam, J., Störzer, H., Shaviv, G., & Wehrse, R. 1988, *A&A*, 193, L1
- Akizuki, C., & Fukue, J. 2007, *PASJ*, submitted
- Artemova, I. V., Bisnovaty-Kogan, G. S., Björnsson, G., & Novikov, I. D. 1996, *ApJ*, 456, 119
- Chandrasekhar, S. 1960, *Radiative Transfer* (New York: Dover Publishing, Inc.)
- Cannizzo, J. K., & Wheeler, J. C. 1984, *ApJS*, 55, 367
- Davis, S. W., Blaes, O. M., Hubeny, I., & Turner, N. J. 2005, *ApJ*, 621, 372
- Dullemond, C.P. 1999, *A&A*, 343, 1030
- Eggum, G. E., Coroniti, F. V., & Katz, J. I. 1985, *ApJ*, 298, L41
- Eggum, G. E., Coroniti, F. V., & Katz, J. I. 1988, *ApJ*, 330, 142
- Fukue, J. 2000, *PASJ*, 52, 829
- Fukue, J. 2004, *PASJ*, 56, 181
- Fukue, J. 2005a, *PASJ*, 57, 841
- Fukue, J. 2005b, *PASJ*, 57, 1023
- Fukue, J. 2006a, *PASJ*, 58, 187
- Fukue, J. 2006b, *PASJ*, 58, 461
- Fukue, J., & Akizuki, C. 2006a, *PASJ*, 58, 1039
- Fukue, J., & Akizuki, C. 2006b, *PASJ*, 58, 1073
- Hubeny, I. 1990, *ApJ*, 351, 632
- Hubeny, I., & Hubeny, V. 1997, *ApJ*, 484, L37
- Hubeny, I., & Hubeny, V. 1998, *ApJ*, 505, 558
- Hubeny, I., Agol, E., Blaes, O., & Krolik, J. H. 2000, *ApJ*, 533, 710
- Hubeny, I., Blaes, O., Krolik, J. H., & Agol, E. 2001, *ApJ*, 559, 680
- Hui, Y., Krolik, J. H. & Hubeny, I. 2005, 625, 913
- Kato, S., Fukue, J., & Mineshige, S. 1998, *Black-Hole Accretion Disks* (Kyoto: Kyoto University Press)
- Križ, S., & Hubeny, I. 1986, *BAIC*, 37, 129
- Levermore, C.D., Pomraning, G.C. 1981, *ApJ*, 248, 321
- Meyer, F., & Meyer-Hofmeister, E. 1982, *A&A*, 106, 34
- Mihalas, D. 1970, *Stellar Atmospheres* (San Francisco: W.H. Freeman and Co.)
- Mihalas, D., & Mihalas, B.W. 1984, *Foundations of Radiation Hydrodynamics* (Oxford: Oxford University Press)
- Mineshige, S., & Wood, J. H. 1990, *MNRAS*, 247, 43
- Narayan, R., & Yi, I. 1994, *ApJ*, 428, L13
- Nobili, L., Turolla, R., & Zampieri, L. 1991, *ApJ*, 383, 250
- Ohsuga, K., Mori, M., Nakamoto, T., & Mineshige, S. 2005, *ApJ*, 628, 368
- Ohsuga, K. 2006, *ApJ*, 640, 923
- Okuda, T. 2002, *PASJ*, 54, 253
- Okuda, T., & Fujita, M. 2000, *PASJ*, 52, L5
- Okuda, T., Fujita, M., & Sakashita, S. 1997, *PASJ*, 49, 679
- Okuda, T., Teresi, V., Toscano, E., & Molteni, D. 2005, *MNRAS*, 357, 295
- Ross, R. R., Fabian, A. C., & Mineshige, S. 1992, *MNRAS*, 258, 189
- Rybicki, G.B., & Lightman, A.P. 1979, *Radiative Processes in Astrophysics* (New York: John Wiley & Sons)
- Shaviv, G., & Wehrse, R. 1986, *A&A*, 159, L5
- Shakura, N. I., & Sunyaev, R. A. 1973, *A&A*, 24, 337
- Shimura, T., & Takahara, F. 1993, *ApJ*, 440, 610
- Shu, F.H. 1991, *The Physics of Astrophysics Vol. 1: Radiation* (California: University Science Books)
- Turolla, R., & Nobili, L. 1988, *MNRAS*, 235, 1273
- Turolla, R., Zampieri, L., & Nobili, L. 1995, *MNRAS*, 272, 625
- Yin, W.-W., & Miller, G. 1995, *ApJ*, 826, 838